FFEMS Fatigue & Fracture of Engineering Materials & Structures
SPECIAL ISSUE CONTRIBUTION
doi: 10.1111/ffe.12156

Prediction of notch sensitivity effects in fatigue and in environmentally assisted cracking

J. T. P. DE CASTRO[1], R. V. LANDIM[2], J. C. C. LEITE[3] and M. A. MEGGIOLARO[1]

[1]*Mechanical Engineering Department, Pontifical Catholic University of Rio de Janeiro (PUC-Rio), Rio de Janeiro, Brazil,* [2]*Instituto Nacional de Tecnologia, INT, Rio de Janeiro, Brazil,* [3]*Petrobras, Macaé, Brazil*

Received Date: 26 September 2013; Accepted Date: 8 January 2014; Published Online: 7 March 2014

ABSTRACT Semi-empirical notch sensitivity factors q have been used for a long time to quantify notch effects in fatigue design. Recently, this old concept has been mechanically modelled using sound stress analysis techniques, which properly consider the notch tip stress gradient influence on the fatigue behaviour of mechanically short cracks. This mechanical model properly calculates q values from the basic fatigue properties of the material, its fatigue limit and crack propagation threshold, considering all the characteristics of the notch geometry and of the loading, without the need for any adjustable parameter. This model's predictions have been validated by proper tests, and a criterion to accept tolerable short cracks has been proposed based on it. In this work, this criterion is extended to model notch sensitivity effects in environmentally assisted cracking conditions.

Keywords environmental effects; non-propagating cracks; notch sensitivity; short cracks.

NOMENCLATURE

a = crack size
a_0 = short crack characteristic size at $R = 0$
a_R = short crack characteristic size at $R \neq 0$
b = notch depth
E = Young's modulus
gr = grain size
K_f = $1 + q(K_t - 1)$, actual value of the stress concentration factor under fatigue loads
K_{max}, K_{min} = maximum and minimum values of the stress intensity factor
K_t = stress concentration factor
K_{tSCC} = $1 + q_{SCC}(Kt - 1)$, actual value of stress concentration factor under stress corrosion cracking conditions
K_{ISCC} = resistance to crack propagation under stress corrosion cracking conditions
pz = plastic zone
q = notch sensitivity factor in fatigue
q_{SCC} = notch sensitivity factor under stress corrosion cracking conditions
R = load ratio, $R = K_{min}/K_{max} = \sigma_{min}/\sigma_{max}$
S_L = fatigue limit amplitude
S_{SCC} = resistance to crack initiation under stress corrosion cracking conditions
S_U = ultimate strength
S_Y = yield strength
γ = Bazant's exponent
ΔK = stress intensity range
ΔK_{tb0} = $\Delta K_{tb}(R = 0)$, long crack fatigue crack growth threshold at $R = 0$
ΔK_{tbR} = $\Delta K_{tb}(R)$, long crack fatigue crack growth threshold at $R \neq 0$
$\Delta K_{tbR}(a)$ = short crack fatigue crack growth threshold at R, a function of the crack size a
ΔS_{L0} = range of the fatigue limit at $R = 0$
ΔS_{LR} = $\Delta S_L(R) = 2S_{LR}$, range of the fatigue limit at $R \neq 0$

Correspondence: J. T. P. de Castro. E-mail: jtcastro@puc-rio.br

$\Delta S_L^{'}(R)$ = range of the fatigue limit at R of standard unnotched and polished specimens
$\Delta\sigma$ = stress range
η = free surface effect on K_I
ρ = notch tip radius
σ = normal stress
σ_{max}, σ_{min} = maximum and minimum values of the stress
vac = subscript denoting vacuum conditions
σ_n = nominal stress
$\varphi(a)$ = effect of the stress gradient near a notch root on K_I

INTRODUCTION

Fatigue damage is associated to two driving forces, one related to cyclic and the other to static damage mechanisms. In this way, fatigue crack growth (FCG) rates on any given environment depend on ΔK and K_{max}, the stress intensity factor (SIF) range and maximum, or on any other pair of parameters related to them. In fact, it is more usual to use ΔK and $R = K_{min}/K_{max}$ to describe and model FCG problems. Even though R is not a crack driving force, such definitions are convenient from an operational point of view because they are easier to compare with familiar notch sensitivity concepts long used by engineers, which this paper aims to improve.

To propagate long cracks by fatigue under fixed $\{\Delta K, K_{max}\}$ or $\{\Delta K, R\}$ loading conditions, the applied SIF range ΔK must be higher than the FCG threshold at the given R ratio, $\Delta K_{th}(R) = \Delta K_{thR}$. Cracks may be considered *short* while their FCG thresholds are smaller than the long crack FCG threshold, thus while such cracks can grow under $\Delta K < \Delta K_{thR}$. This behaviour is natural, because otherwise the stress ranges $\Delta\sigma$ required to propagate short cracks at a given R would be higher than their fatigue limits $\Delta S_L(R) = \Delta S_{LR}$, the stress range needed to initiate and propagate cracks in smooth specimens at that R ratio. Indeed, assuming as usual that at any given fixed R ratio, the FCG process is driven by the SIF range $\Delta K \propto \Delta\sigma\sqrt{(\pi a)}$, if very short cracks with size $a \to 0$ had the same ΔK_{thR} threshold the long cracks have, they would need $\Delta\sigma \to \infty$ to grow by fatigue, a meaningless requirement.[1–3] Such statements assume that the stresses are induced only by external loads; but if the cracks start from notch tips or from smooth surfaces previously subjected to plastic strain gradients or to any other source that can induce residual stress fields, these resident stresses must be added to the externally applied stresses as static loading components that affect R but not ΔK.

Microstructurally short cracks, those small compared with the grain size gr, are much affected by microstructural barriers such as grain boundaries; hence, cannot be well modelled for structural design purposes using macroscopic stress analysis techniques and isotropic properties.[4–9]

Mechanically short cracks, on the other hand, with sizes $a > gr$, may be modelled by Linear Elastic Fracture Mechanics (LEFM) concepts if the stress field that surrounds them is predominantly Linear Elastic, and if the material can be treated as isotropic and homogeneous in such a scale. Because near-threshold FCG is always associated with small-scale yielding conditions, to check if short cracks really may be modelled in such a way, the idea is to follow Irwin's steps by first assuming that such concepts are valid and then verifying if their predictions are validated by proper tests. Hence, in the sequence, first LEFM techniques are used to develop a model for the FCG behaviour of mechanically short cracks, in particular those that depart from notches, and then the notch sensitivity predictions based on it are corroborated by proper experiments. Finally, such concepts are extended to model notch sensitivity effects under environmentally assisted cracking (EAC) conditions.

THE BEHAVIOUR OF SHORT CRACKS IN FATIGUE

To reconcile the traditional fatigue (crack initiation) limit, $\Delta S_{L0} = 2S_L(R = 0)$, with the FCG threshold of long cracks under pulsating loads, $\Delta K_{th0} = \Delta K_{th}(R = 0)$, Topper and his colleagues[10–12] added to the physical crack size a hypothetical *short crack characteristic size* a_0, a wise stratagem that forces the SIF of all cracks, short or long, to obey the correct FCG limits:

$$\Delta K_I = \Delta\sigma\sqrt{\pi(a + a_0)}, \text{ where } a_0 = (1/\pi)(\Delta K_{th0}/\Delta S_{L0})^2. \quad (1)$$

In this way, long cracks with $a \gg a_0$ (in Griffith's plates under pulsating loads) do not grow by fatigue if $\Delta K_I = \Delta\sigma\sqrt{(\pi a)} < \Delta K_{th0}$, whereas very small cracks with $a \to 0$ do not grow if $\Delta\sigma < \Delta S_{L0}$, because $\Delta K_I = \Delta\sigma\sqrt{(\pi a_0)} < S_{L0}\sqrt{(\pi a_0)} = \Delta K_{th0}$ in this case. Moreover, this clever idea reproduces the whole tendency of typical $\Delta\sigma_j \times a_j$ data points in Kitagawa–Takahashi diagrams, where $\Delta\sigma_j$ is the stress range needed to propagate a fatigue crack with size a_j, see Fig. 1.[13] This figure also shows the fatigue

limit ΔS_{L0} and the stress range $\Delta\sigma(a) = \Delta K_{th0}/\sqrt{(\pi a)}$ associated to the long crack threshold, which limit the region that may contain non-propagating cracks, as well as the El Haddad–Topper–Smith (ETS) curve, which predicts that cracks of any size should stop when

$$\Delta\sigma(a) \leq \Delta K_{th0}/\sqrt{\pi(a+a_0)}. \quad (2)$$

Steels typically have $6 < \Delta K_{th0} < 12\,\text{MPa}\sqrt{\text{m}}$, ultimate tensile strengths $400 < S_U < 2000\,\text{MPa}$, and fatigue limits $200 < S_L < 1000\,\text{MPa}$ (the best high-strength steels with very clean microstructures tend to maintain the trend $S_L \cong S_U/2$ for smooth test specimens). Consequently, the range of their fatigue limits under pulsating loads (those with $R = 0$) estimated by Goodman is

$$\Delta S_{L0} \cong 2S_U S_L/(S_U + S_L) \Rightarrow 260 < \Delta S_{L0} < 1300\,\text{MPa}. \quad (3)$$

Hence, the range of characteristic short crack sizes in steel components (in large plates with a central crack subject to pulsating tensile loads) estimated according to the ETS model is

$$(1/\pi)\cdot(\Delta K_{th0_{min}}/\Delta S_{L0_{max}})^2 \cong 7 < a_0 < 700\mu m \cong (1/\pi)\cdot(\Delta K_{th0_{max}}/\Delta S_{L0_{min}})^2. \quad (4)$$

Because such a_0 values are small, the denomination 'short crack characteristic size' is justifiable. Indeed, they hardly reach the detection thresholds of traditional non-destructive inspection methods [14]. For typical Al alloys (with $30 < S_L < 230\,\text{MPa}$, $70 < S_U < 600\,\text{MPa}$, $40 < \Delta S_{L0} < 330$ MPa and $1.2 < \Delta K_{th0} < 5\,\text{MPa}\sqrt{\text{m}}$), the range estimated for a_0 is a little larger, $1\,\mu\text{m} < a_0 < 5\,\text{mm}$. So, it can be expected that short crack effects on materials with high ΔK_{th0} and low ΔS_{L0} to be more pronounced in Al alloys than in steels. Note, however, that such values assume a through-thickness one-dimensional (1D) crack, one that can be completely described by just one size parameter. Most such small cracks probably should be better treated as two-dimensional (2D) cracks as discussed latter on; but to explain such concepts, this unidimensional analysis is certainly more appropriate. Moreover, as the generic SIF of cracked structural components is given by $K_I = \sigma\sqrt{(\pi a)}\cdot g(a/w)$, Yu, Duquesnay and Topper[12] used the geometry factor $g(a/w)$ to generalize Eq. (1) and redefined the short crack characteristic size by

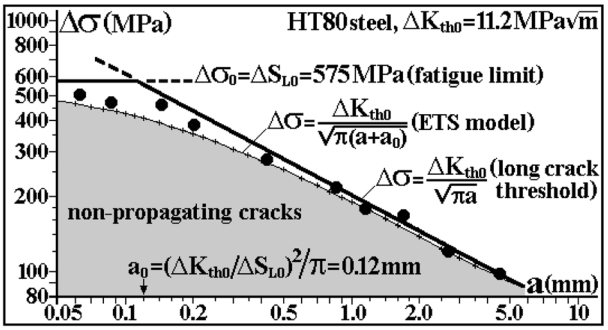

Fig. 1 Stress ranges $\Delta\sigma(a)$ required to propagate cracks of size a under $R = 0$ in an HT80 steel plate with $\Delta K_{th0} = 11.2\,\text{MPa}\sqrt{\text{m}}$ and $\Delta S_{L0} = 575$ MPa: long cracks, with $a \gg a_0$, stop when $\Delta\sigma \leq \Delta K_{th0}/\sqrt{(\pi a)}$; whereas very short cracks, with $a \to 0$, stop when $\Delta\sigma \leq \Delta S_{L0}$. The El Haddad–Topper–Smith model predicts that any crack should stop when $\Delta\sigma \leq \Delta K_{th0}/\sqrt{[\pi(a+a_0)]}$.

$$\Delta K_I = \Delta\sigma\sqrt{\pi(a+a_0)}\cdot g(a/w), \text{where } a_0 = (1/\pi)\cdot\left(\Delta K_{th0}/\left[\Delta S_{L0}\cdot g(a/w)\right]\right)^2. \quad (5)$$

The largest stress range $\Delta\sigma$ that does not propagate microcracks in this case is also the fatigue limit, as it should: if $a \ll a_0$, $\Delta K_I = \Delta K_{th0} \Rightarrow \Delta\sigma \to \Delta S_{L0}$. However, when the crack starts from a notch, as usual, its driving force is the stress range $\Delta\sigma$ at the notch root, not the nominal stress range $\Delta\sigma_n$ normally used in SIF expressions. As in such cases, the $g(a/w)$ factor includes the stress concentration effect of the notch, it is better to split it into two parts: $g(a/w) = \eta\cdot\varphi(a)$, where $\varphi(a)$ quantifies the effect of the stress gradient near the notch root, which for microcracks tend towards K_t, that is, $\varphi(a \to 0) \to K_t$, whereas the constant η quantifies the effect of the other parameters that affect K_I, such as the free surface. In this way, it is better to define a_0 by

$$\Delta K_I = \eta\cdot\varphi(a)\cdot\Delta\sigma_n\sqrt{\pi(a+a_0)}, \text{where } a_0 = (1/\pi)\cdot[\Delta K_{th0}/(\eta\cdot\Delta S_{L0})]^2. \quad (6)$$

The stress gradient effect quantified by $\varphi(a)$ does not affect a_0 because the stress ranges at notch tips must be smaller than the fatigue limit to avoid crack initiation, $\Delta\sigma(a \to 0) = K_t\Delta\sigma_n = \varphi(0)\Delta\sigma_n < \Delta S_{L0}$. However, because SIFs are crack driving forces, they should be material independent. Hence, the a_0 effect on the short crack behaviour should be used to modify the FCG thresholds instead of the SIF, making them a function of the crack size, a trick that is quite convenient for operational reasons. In this way, the a_0-dependent FCG threshold for pulsating loads $\Delta K_{th}(a, R = 0) = \Delta K_{th0}(a)$ becomes

$$\frac{\Delta K_{th0}(a)}{\Delta K_{th0}} = \frac{\Delta\sigma\sqrt{\pi a}\cdot g(a/w)}{\Delta\sigma\sqrt{\pi(a+a_0)}\cdot g(a/w)} = \sqrt{\frac{a}{a+a_0}} \Rightarrow \Delta K_{th0}(a) = \Delta K_{th0}[1 + (a_0/a)]^{-1/2}. \quad (7)$$

Note that for $a \gg a_0$ this short crack FCG threshold tends to ΔK_{th0}, the traditional long crack FCG threshold, and becomes independent of the crack size, as it should.

It may be convenient to assume that Eq. (7) is just one of the models that obey the long crack and the short crack limit behaviours, introducing in the $\Delta K_0(a)$ definition a data fitting parameter γ proposed by Bazant[15] to obtain

$$\Delta K_{th0}(a) = \Delta K_{tb0}\left[1 + (a_0/a)^{\gamma/2}\right]^{-1/\gamma}. \quad (8)$$

Equation (8) reproduces the original ETS model when $\gamma = 2$, as well as the bilinear limits shown in Fig. 1, $\Delta\sigma = \Delta S_{L0}$ and $\Delta\sigma = \Delta Kth_0/\sqrt{(\pi a)}$, when $\gamma \to \infty$. This additional parameter may allow a better fitting of experimental data, such as those collected by Tanaka *et al.*[16] and by Livieri and Tovo,[17] as shown in Fig. 2: most data on short cracks are contained by the curves generated using $\gamma = 1.5$ and $\gamma = 8$. The curves shown in Fig. 3 illustrate the influence of γ on the minimum stress ranges needed to propagate short or long cracks under pulsating loads as a function of the crack size a:

$$\Delta\sigma_0(a) = \left[\Delta K_{tb0}/\sqrt{\pi a}\right]\cdot\left[(1 + a/a_0)^{\gamma/2}\right]^{-1/\gamma}. \quad (9)$$

However, because fatigue damage depends on two driving forces, ΔK and K_{max}, as explained in the introduction, Eq. (8) should be extended to consider the σ_{max} influence (indirectly modelled by the R ratio) on the short crack behaviour. Thus, if $\Delta K_{tbR} = \Delta K_{tbR}(a \gg a_R, R)$ is the FCG threshold for long cracks, $\Delta S_{LR} = \Delta S_L(R)$ is the fatigue limit at the desired R ratio, and a_R is the characteristic short crack size at R, then

$$\Delta K_{thR}(a) = \Delta K_{tbR}\cdot\left[1 + (a_R/a)^{\gamma/2}\right]^{-1/\gamma}, \text{where}$$
$$a_R = (1/\pi)[\Delta K_{tbR}/(\eta\cdot\Delta S_{LR})]^2. \quad (10)$$

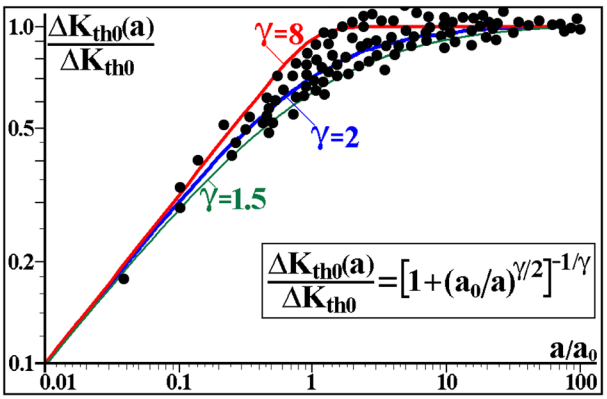

Fig. 2 The additional parameter γ in $\Delta K_{th0}(a)/\Delta K_{tb0} = [1 + (a_0/a)^{\gamma/2}]^{-1/\gamma}$ may allow a better fitting of the short crack FCG thresholds measured experimentally.

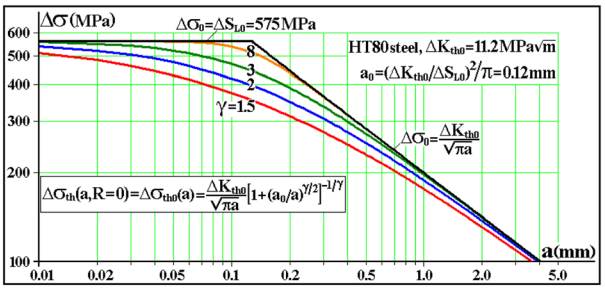

Fig. 3 Influence of γ in the fatigue limit curves $\Delta\sigma_0(a)$ predicted by Eq. (9): the larger the γ value is, the faster $\Delta\sigma_0(a)$ tends to the bilinear limit defined by $\Delta\sigma_0 = \Delta K_{tb0}/\sqrt{(\pi a)}$, the fatigue crack growth threshold under pulsating loads for long cracks with size $a \gg a_0$, and to $\Delta\sigma_0 = \Delta S_{L0}$, the fatigue limit under pulsating stresses for very small cracks with $a \ll a_0$.

Albeit defect-free microfilaments (whiskers) can be made in lab conditions, structural components used in practice always contain tiny defects such as inclusions, voids and scratches, which behave as small cracks. If the size of such defects is not much smaller than a_0, the structural effects of such (mechanically) short cracks can be evaluated using LEFM concepts, as follows.[17–27]

INFLUENCE OF SHORT CRACKS ON THE FATIGUE LIMIT OF STRUCTURAL COMPONENTS

Traditional SN and εN methods are used to analyse and design supposedly crack-free components. However, as it is impossible to guarantee that they are really free of cracks smaller than the detection threshold of the non-destructive method used to inspect them, SN or εN predictions may become unreliable when such tiny defects are introduced by any means during their manufacture or service. Hence, structural components should be designed to tolerate undetectable short cracks.

Despite self-evident, this prudent requirement is still not included in most fatigue design routines, which just intend to maintain the service stresses at critical points below their fatigue limits, $\Delta\sigma < \Delta S_{LR}/\varphi_F$, where φ_F is a suitable safety factor. Nevertheless, most long-life designs work just fine, thus they are somehow tolerant to undetectable or to functionally admissible short cracks. But the question 'how much tolerant' cannot be answered by SN or εN procedures alone. Such problems can be avoided by adding a tolerance to short crack requirement to their 'infinite' life design criteria, which, in its simplest version, may be given by

$$\Delta\sigma \le \Delta K_{thR}/\left\{\varphi_F\cdot\sqrt{\pi a}\cdot g(a/w)\cdot\left[1 + (a_R/a)^{\gamma/2}\right]^{1/\gamma}\right\}, \quad (11)$$
$$a_R = (1/\pi)[\Delta K_{thR}/(\eta\Delta S_{LR})]^2.$$

Because the fatigue limit ΔS_{LR} already reflects the effect of microstructural defects that are inherent to the material, Eq. (11) complements it by describing the tolerance to cracks of size a (small or not) that may pass unnoticed in actual service conditions. Such estimates can be very useful for designers and quality control engineers. They can be used as a quantitative tool to evaluate the effect of accidental damages to the surface of otherwise well-behaved components, but they have some limitations. They assume that the short crack grows unidimensionally (1D), thus can be characterized by its size a only. However, as the short cracks frequently are small compared with the structural component dimensions, they are better described as 2D cracks that grow by fatigue in two directions maintaining their original plane under mode I loads, but usually changing their shape at every load cycle. Moreover, such estimates are valid for mechanically but not for microstructurally short cracks, that is, they are valid for cracks with both a and a_0 larger than the grain size gr. The local FCG behaviour of microcracks with size $a < gr$ is sensitive to microstructural features such as the grain orientation and cannot be properly modelled using macroscopic material properties. Such problems have academic interest,[4–9] but as the grains still cannot be mapped in practice, they cannot be properly used for structural engineering applications yet.

To model short 2D (mechanical) cracks that tend to grow both in depth and width in the simplest possible way, it is assumed that: (i) the cracks are loaded in pure mode I under quasi-constant $\Delta\sigma$ and R conditions, with no overloads or any other event capable of inducing load sequence effects; (ii) material properties measured testing 1D cracks in standard specimens such as ΔK_{thR} may be used to simulate FCG or stress corrosion cracking (SCC) behaviour of 2D cracks; and (iii) 2D surface or corner cracks can be well modelled as having an approximately elliptical front, thus their SIF can be described by the classical Newman–Raju equations.[26,28–30] If such reasonable hypotheses hold as expected, then the structural components tolerance to short or long fatigue cracks are given by

$$\Delta\sigma < \begin{cases} \Delta K_{thR} \Big/ \left\{ \sqrt{\pi a}\cdot\Phi_a(a,c,w,t)\cdot\left[1+(a_R/a)^{\gamma/2}\right]^{1/\gamma} \right\} \\ \Delta K_{thR} \Big/ \left\{ \sqrt{\pi c}\cdot\Phi_c(a,c,w,t)\cdot\left[1+(a_R/c)^{\gamma/2}\right]^{1/\gamma} \right\} \end{cases} \tag{12}$$

The mode I SIFs at the tips of the semi-axes a along the depth and c along the width of semi-elliptical surface cracks in a plate of width $2w$ and thickness t loaded under a pure tensile nominal load σ are $K_I(a) = \sigma\sqrt{(\pi a)}\cdot\Phi_a = \sigma\sqrt{(\pi a)}\cdot F\cdot M/Q^{0.5}$ and $K_I(c) = \sigma\sqrt{(\pi a)}\cdot\Phi_c = \sigma\sqrt{(\pi a)}\cdot(F\cdot M/Q^{0.5})\cdot(a/c)\cdot G$ for $a < t$ and $c < w$ (Eq. (13)). The similar mode I SIFs for quarter-elliptical corner cracks are even more complex.[28] Such complex 2D SIFs enhance the operational advantage of treating the FCG threshold as a function of the crack size, $\Delta K_{thR}(a)$.

$$\begin{cases} K_I(a) = \sigma\sqrt{\pi a}\cdot F\cdot M/\sqrt{Q} \\ K_I(c) = \sigma\sqrt{\pi c}\cdot F\cdot\left(M/\sqrt{Q}\right)\cdot a/c\cdot G \\ F(c/w,a/t) = \sqrt{\sec\left[(\pi c/2w)\sqrt{a/t}\right]}\cdot\left[1-0.025\left[(c/w)\sqrt{a/t}\right]^2+0.06\left[(c/w)\sqrt{a/t}\right]^4\right] \\ M = \begin{cases} 1.13-0.09\dfrac{a}{c}+\left[\dfrac{0.89}{0.2+a/c}-0.54\right]\dfrac{a^2}{t^2}+\left[0.5-\dfrac{1}{0.65+a/c}+14\left(1-\dfrac{a}{c}\right)^{24}\right]\dfrac{a^4}{t^4}, & a\le c \\ c/a+0.04(c/a)^2+(c/a)^{4.5}(a/t)^2\left[0.2-0.11(a/t)^2\right], & a>c \end{cases} \\ Q = \begin{cases} 1+1.464(a/c)^{1.65}, & a\le c \\ 1+1.464(c/a)^{1.65}, & a>c \end{cases}, \quad G = \begin{cases} 1.1+0.35(a/t)^2, & a\le c \\ 1.1+0.35(a/t)^2(c/a), & a>c \end{cases} \end{cases} \tag{13}$$

However, if the short 2D cracks start from notch tips, as usual, the stress analysis problem may be still more complex. In general, they must include non-negligible 3D gradient effects around the notch tips, as discussed elsewhere.[29] On the other side, the tolerance to SCC cracks can be treated using these same principles, by properly changing the fatigue properties ΔK_{thR} and ΔS_{LR} by the corresponding material resistances to SCC cracking in the desired environment, K_{ISCC} and S_{SCC}, as explained later on.

ANALYSIS OF NOTCH SENSITIVITY EFFECTS ON FATIGUE

The SIF of small mechanical cracks that start at the roots of notches with depth b and tip radius ρ can be estimated by $K_I \cong 1.12\sigma_n \cdot f_1(K_t, a)\sqrt{(\pi a)}$, where $f_1 = \sigma_y(x)/\sigma_n$ is the stress concentration perpendicular to the crack plane at the point $(x = b + a, y = 0)$ ahead of such tips. The stress concentration effect of such notches can be estimated by an ellipse with semi-axes b and c and notch tip radius $\rho = c^2/b$. If the ellipse axis $2b$ is centred at the x-axis origin and is perpendicular to the nominal stress σ_n, then[31]

$$f_1 = \frac{\sigma_y(x = b + a, y = 0)}{\sigma_n} = 1 + \frac{(b^2 - 2bc)\left(x - \sqrt{x^2 - b^2 + c^2}\right)\left(x^2 - b^2 + c^2\right) + bc^2(b - c)x}{(b - c)^2\left(x^2 - b^2 + c^2\right)\sqrt{x^2 - b^2 + c^2}}. \quad (14)$$

The high stress gradient ahead of elongated notch tips justifies the peculiar behaviour of short cracks that start from sharp notches: in the Linear Elastic case, the tangential stress at x = 1.2b ahead *any* elliptical hole with $b \geq c$ is $\sigma_y(1.2, 0)/\sigma_n \cong 2$, independently of the elliptical notch stress concentration factor (SCF) K_t. As the stress gradient around sharp notch tips is high, the SIF induced by remotely applied loads on short cracks that start there first grows fast with their growing sizes a, but after a small Δa increment they may stabilize or even decrease their rates for a while before growing once again, since the notch effect on K_I may diminish sharply as the short crack grows. Indeed, the term $\sqrt{a}$ that increases $K_I = 1.12\sigma\sqrt{(\pi a)} \cdot f_1$ can be overcompensated by the abrupt fall in f_1 near the notch tip (Fig. 4). Such simple concepts can be used to evaluate the tolerance to fatigue cracks that start from such notches by using the $K_I(a)$ and $\Delta K_{thR}(a)$ estimates for the crack SIF and for the FCG threshold of the material[26]. In other words, short cracks can be arrested whenever their SIFs, which are highly sensitive to the stress gradient ahead of the notch tips, become smaller than the short crack FCG threshold at the given R ratio, which depends on the crack size a, whereas it is not much larger than the characteristic short crack size a_R: $\Delta K_I(a) \leq \Delta K_{thR}(a) \Rightarrow$ crack arrest.

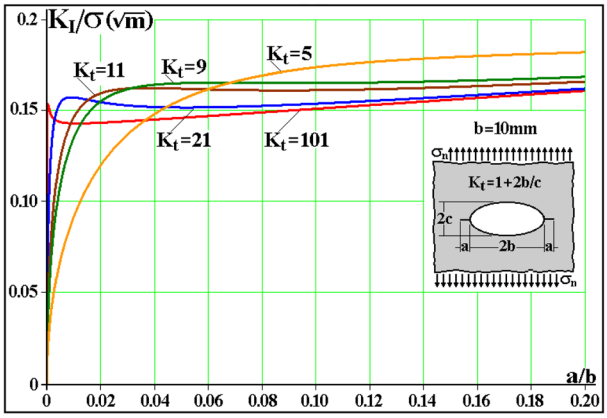

Fig. 4 $K_I \cong 1.12 \cdot \sigma_n \sqrt{(\pi a)} \cdot f_1(K_t, a)$ estimate for small cracks $a \leq b/5$ that start from the tips of several Inglis holes with b = 10mm.

The notch sensitivity q still is quantified for design purposes by empirical curves fitted to only seven experimental points compiled by Peterson[32] a long time ago. It is used to estimate fatigue limits measured under fixed $\Delta\sigma_n$ and R in notched test specimens with a SCF $K_t \geq K_f = 1 + q \cdot (K_t - 1)$ by $\Delta S_{LR} = \Delta S_L'(R)/K_f$, where ΔS_{LR} is the fatigue limit of the notched test specimens, and $\Delta S_L'(R)$ is the unnotched fatigue limit under the same R ratio.

However, according to Frost,[33] early data showing that small non-propagating fatigue cracks are found at notch tips when $\Delta S_{LR}/K_t < \Delta\sigma_n < \Delta S_{LR}/K_f$ goes back as far as 1949. It is thus reasonable to expect that q is related to the fatigue behaviour of short cracks emanating from notch tips or that such tiny cracks can be used to quantify $K_f \leq K_t$ values. The notch sensitivity can in fact be calculated in this way using relatively simple but sound mechanical principles that do not require heuristic arguments, neither arbitrary fitting parameters. To start with, according to Tada,[34] the SIF of a crack with size a that departs from a circular hole of radius ρ is given within 1% by

$$\begin{cases} K_I = 1.1215 \cdot \sigma\sqrt{\pi a} \cdot \varphi(x), \quad x \equiv a/\rho \\ \varphi(x) = \left[1 + \dfrac{0.2}{(1+x)} + \dfrac{0.3}{(1+x)^6}\right] \cdot \left[2 - 2.354 \cdot \left(\dfrac{x}{1+x}\right) + 1.206 \cdot \left(\dfrac{x}{1+x}\right)^2 - 0.221 \cdot \left(\dfrac{x}{1+x}\right)^3\right] \end{cases} \quad (15)$$

Note that when $a \to 0 \Rightarrow x \to 0$, this equation tends to the expected limit,

$$\lim_{a \to 0} \Delta K_I = 1.1215 \cdot 3 \cdot \Delta\sigma\sqrt{\pi a}. \quad (16)$$

Indeed, this equation combines the solution for an edge crack in a semi-infinite plate with the SCF of the Kirsch hole, $K_t = 3$. Note also that it reproduces the correct limit once again when $a \to \infty$, the SIF of an Irwin's plate with a crack of length a (in fact, $a + 2\rho \cong a$, as in this case $a \gg \rho$) because the crack tip is so distant from the hole that it is not affected by it:

$$\lim_{a\to\infty} \Delta K_I = \Delta\sigma\sqrt{\pi a/2}. \tag{17}$$

Hence, for Kirsch holes such limits are $\varphi(x = 0) = 3$ and $\varphi(x \to \infty) = 1/1.1215\sqrt{2} \cong 0.63$. The FCG condition for cracks that start at such notch borders under pulsating loads is thus

$$\begin{aligned}\Delta K_I &= \Delta\sigma\sqrt{\pi a}\cdot\eta\cdot\varphi(a/\rho) > \Delta K_{tb0}(a)\\ &= \Delta K_{tb0}\cdot\left[1 + (a_0/a)^{\gamma/2}\right]^{-1/\gamma}\end{aligned} \tag{18}$$

where $\Delta K_{tb0} = \Delta S_{L0}\sqrt{(\pi a_0)} \equiv \Delta K_{tb0}(a \gg a_0)$, and $a_0 = (1/\pi)[\Delta K_{tb0}/(\eta\cdot\Delta S_{L0})]^2$. Note that a_0 cannot depend on the stress gradient factor $\varphi(a/w)$, otherwise it would not be a material property. This FCG criterion can be rewritten using two dimensionless functions, one related to the notch stress gradient $\varphi(a/\rho)$, and the other $g(\Delta S_{L0}/\Delta\sigma, a/\rho, \Delta K_{tb0}/\Delta S_{L0}\sqrt{\rho}, \gamma)$, which includes the effects of the applied stress range $\Delta\sigma$, the crack size a, the notch tip radius ρ, the fatigue resistances ΔS_{L0} and ΔK_{tb0}, and the optional data fitting exponent γ (if it is used):[25]

$$\begin{aligned}\varphi(a/\rho) &> \frac{(\Delta S_{L0}/\Delta\sigma)\cdot\left[\Delta K_{tb0}/\left(\Delta S_{L0}\sqrt{\rho}\right)\right]}{\left[\left(\eta\sqrt{\pi a/\rho}\right)^{\gamma} + \left[\Delta K_{tb0}/\left(\Delta S_{L0}\sqrt{\rho}\right)\right]^{\gamma}\right]^{1/\gamma}}\\ &\equiv g\left(\frac{\Delta S_{L0}}{\Delta\sigma}, \frac{a}{\rho}, \frac{\Delta K_{tb0}}{\Delta S_{L0}\sqrt{\rho}}, \gamma\right).\end{aligned} \tag{19}$$

Therefore, if $x \equiv a/\rho$ and $\kappa \equiv \Delta K_{tb0}/(\Delta S_{L0}\sqrt{\rho}) = \eta\cdot\sqrt{(\pi a_0/\rho)}$, a fatigue crack departing from a Kirsch hole under pulsating loads grows whenever $\varphi(x)/g(\Delta S_{L0}/\Delta\sigma, x, \kappa, \gamma) > 1$. Figure 5 plots some φ/g functions for several fatigue strength to loading stress range ratios $\Delta S_{L0}/\Delta\sigma$ as a function of the normalized crack length x for a small notch radius $\rho \cong 1.40a_0$, comparable with the short crack characteristic size, and for $\kappa = \Delta K_{tb0}/[\Delta S_{L0}\sqrt{(1.4a_0)}] = 1.12\sqrt{(\pi/1.4)} = 1.68$ and $\gamma = 6$.[26]

For high applied stress ranges $\Delta\sigma$, the strength to load ratio $\Delta S_{L0}/\Delta\sigma$ is small, and the corresponding φ/g curve is always higher than 1, so cracks will initiate and propagate from this small Kirsch hole border without stopping during this process. One example of such a case is the upper curve in Fig. 5, which shows the function $\varphi/g_{1.4}$ obtained for $\Delta S_{L0}/\Delta\sigma = 1.4$. On the other hand, small stress ranges with load ratios $\Delta S_{L0}/\Delta\sigma \geq K_t = 3$ have $\varphi/g < 1$, meaning

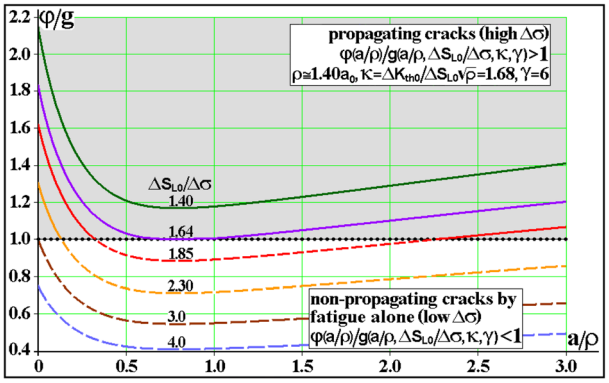

Fig. 5 Cracks that can start from the border of a (small) Kirsch hole with $K_t = 3$ may propagate by fatigue and then stop if their $\varphi/g < 1$ ($\rho \cong 1.40a_0$, $\kappa = 1.68$, and $\gamma = 6$ in this figure).

that such loads cannot initiate a fatigue crack from this hole and that small enough cracks introduced there by any other means will not propagate at such low loads. This is illustrated by curves φ/g_3, associated with the limit case where the local stress range equals the material fatigue strength $\Delta S_{L0}/\Delta\sigma = 3$, and φ/g_4, associated with a still smaller load, $\Delta S_{L0}/\Delta\sigma = 4$.

Three other curves must be analysed in Fig. 5. The $\varphi/g_{2.3}$ curve crosses the $\varphi/g = 1$ line once, meaning that such an intermediate load can initiate and propagate a fatigue crack from this hole border, until the decreasing $\varphi/g_{2.3}$ ratio reaches 1, where the crack stops because the stress gradient ahead of its small tip is sharp enough to eventually force $\Delta K_I(a) < \Delta K_{th}(a)$. Thus, under this $\Delta\sigma = \Delta S_{L0}/2.3$ loading, a non-propagating fatigue crack is generated at this small hole border, with a size given by the corresponding a/ρ abscissa where $\varphi/g_{2.3} = 1$. The $\varphi/g_{1.85}$ curve intersects the $\varphi/g = 1$ line twice. This load level also generates a fatigue crack at the hole border, which will propagate until reaching the maximum size obtained from the abscissa of the first intersection point (on the left in that figure), where the crack stops because it reaches $\Delta K_I(a) < \Delta K_{tb0}(a)$. Moreover, cracks longer than the second intersection point will restart propagating by fatigue under $\Delta\sigma = \Delta S_{L0}/1.85$, until eventually fracturing this Kirsch plate. However, the crack initiated by fatigue under such an intermediate pulsating load range cannot propagate between these two intersection points by fatigue alone, if the loading parameters $\{\Delta\sigma, \sigma_{max}\}$ remain constant. Hence, the crack can only grow in this region if helped by a different damage mechanism, such as SCC or creep.

The FCG behaviour of these two curves seems different in Fig. 5, yet they are similar. Indeed, the $\varphi/g_{2.3}$ curve crosses the $\varphi/g = 1$ line twice if the graph is extended to include larger cracks.[26] This is so because a sufficiently long crack can always propagate by fatigue under any given (even if small) $\Delta\sigma$ range if its SIF range

$\Delta K = \Delta\sigma\sqrt{(\pi a)}\cdot g(a/w)$ grows with the crack size a, as in this Kirsch plate. In fact, all φ/g curves eventually become higher enough for sufficiently large a/ρ values, even those that cannot initiate a crack by fatigue, such as φ/g_4.

Finally, note the $\varphi/g_{1.64}$ curve that is tangent to the $\varphi/=1$ line in Fig. 5. Therefore, this pulsating stress range $\Delta\sigma = \Delta S_{L0}/1.64$ is the smallest one that can cause crack initiation and growth (without arrest) from that notch border by fatigue alone. Hence, by definition, the fatigue SCF of this small Kirsch hole (with $\rho \cong 1.40\cdot a_0$, $\kappa = \eta\cdot\sqrt{(\pi a_0/\rho)} = 1.5$ and $\gamma = 6$) is thus $K_f = 1.64$; therefore, its notch sensitivity factor is $q = (K_f - 1)/(K_t - 1) = (1.64 - 1)/(3 - 1) = 0.32$. Moreover, the abscissa of the tangency point between the $\varphi/g_{1.64}$ curve and the $\varphi/g = 1$ line gives the largest non-propagating crack size that can arise from it by fatigue alone, a_{max}. For any other ρ/a_0, γ and $\kappa = \eta\cdot\sqrt{(\pi a_0/\rho)}$ combination, K_f and a_{max} can always be found by solving the system

$$\begin{cases} \varphi/g = 1 \\ \partial(\varphi/g)/\partial x = 0 \end{cases} \Rightarrow \begin{cases} \varphi(x_{max}) = g(x_{max}, K_f, \kappa, \gamma) \\ \partial\varphi(x_{max})/\partial x = \partial g(x_{max}, K_f, \kappa, \gamma)/\partial x \end{cases} \tag{20}$$

Kirsch (circular) holes cause relatively mild stress gradients. Larger holes compared with the short crack characteristic size, $\rho \gg a_0$, are associated to small $\kappa = \eta\cdot\sqrt{(\pi a_0/\rho)}$ values and do not induce short crack arrest. For example, Kirsch holes with $\rho > 7\cdot a_0$ in a material with $\gamma = 6$ do not induce non-propagating fatigue cracks under fixed pulsating loads, thus have $q = 1$. That is a sound mechanical interpretation for the notch sensitivity concept. If for a given γ Eq. (20) is solved for several notch tip radii ρ using $\kappa \equiv \Delta K_{th0}/\Delta S_{L0}\sqrt{\rho}$, then the notch sensitivity factor q is obtained by

$$q(\kappa, \gamma) \equiv \left[K_f(\kappa, \gamma) - 1\right]/(K_t - 1). \tag{21}$$

This approach has four major assets: (i) it is an analytical procedure; (ii) it considers the effect of the fatigue resistances to crack initiation and propagation on q; (iii) it can use the exponent γ to generalize the original ETS model, but it does not need it neither any other data fitting parameter; and (iv) it can be easily extended to deal with other notch geometries. For example, the SIF of cracks that depart from a semi-elliptical notch with semi-axes b and c, with b in the same direction of the crack a, which is perpendicular to the (nominal) stress $\Delta\sigma$, can be described by:

$$\Delta K_I = \eta\cdot F(a/b, c/b)\cdot\Delta\sigma\sqrt{\pi a} \tag{22}$$

where $\eta = 1.1215$ is the free surface correction factor and $F(a/b, c/b)$ is the geometrical factor associated to the notch stress concentration effect. Such notch SCFs K_t are approximately given by:[34]

$$K_t = (1 + 2b/c)\cdot\left[1 + 0.1215/(1 + c/b)^{2.5}\right]. \tag{23}$$

Using $s = a/(a + b)$, two analytical expressions for $F(a/b, c/b)$ were introduced in Ref. [25] by fitting results obtained by a series of Finite Element (FE) analyses for several types of semi-elliptical notches, made using the QUEBRA2D software,[35] which reproduce very well the results of Nishitani and Tada quoted by Bazant[15] (Fig. 6):

$$\begin{cases} F(a/b, c/b) \equiv f(K_t, s) = K_t\sqrt{\left[1 - \exp\left(-K_t^2\cdot s\right)\right]/\left(K_t^2\cdot s\right)}, & c \le b \\ F(a/b, c/b) \equiv f'(K_t, s) = K_t\sqrt{\dfrac{1 - \exp\left(-K_t^2\cdot s\right)}{K_t^2\cdot s}}\cdot\left[1 - \exp\left(-K_t^2\right)\right]^{-s/2}, & c \ge b \end{cases} \tag{24}$$

Equating $g = \varphi$, the minimum stress range needed to start and propagate a fatigue crack from the edge of such notches can be calculated for several combinations of κ and γ, leading to expressions for K_f and, consequently,

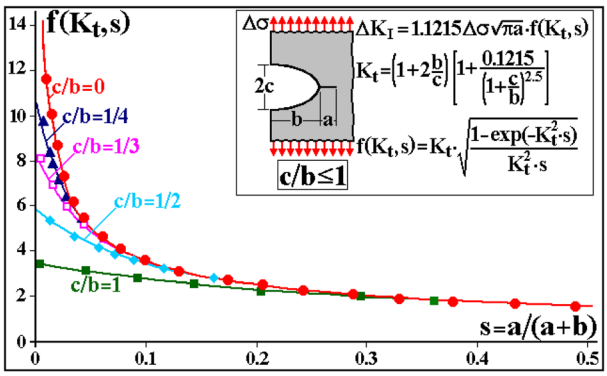

Fig. 6 Stress intensity factors calculated for cracks that depart from semi-elliptical notches with $c \le b$.

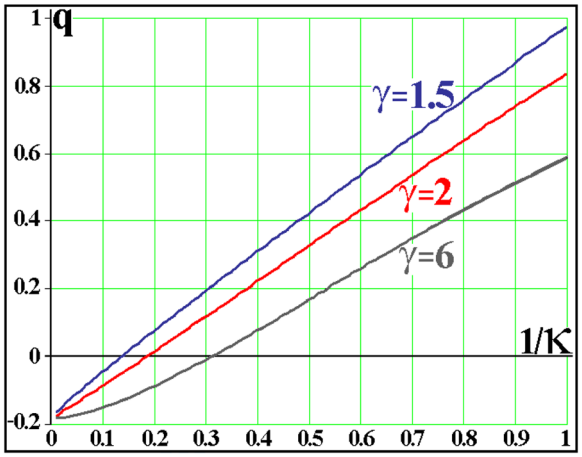

Fig. 7 Notch sensitivity $q(1/\kappa)$ estimated for a (circular) Kirsch hole.

for q (Fig. 7). Note that the notch sensitivity $q(1/\kappa)$ estimated in this way is almost linear for sensitivities $q > 0$; hence, it can be approximately modelled by

$$q(\kappa,\gamma) \cong q_1(\gamma)/\kappa - q_0(\gamma) = q_1(\gamma)\Delta S_{L0}\sqrt{\rho}/\Delta K_{th0} - q_0(\gamma). \tag{25}$$

The parameters $q_0(\gamma)$ and $q_1(\gamma)$ that fit the quasi-linear part of $q(\gamma, \kappa)$ depend only on γ, whereas the parameter $1/\kappa = \Delta S_{L0}\sqrt{\rho}/\Delta K_{th0}$ includes the material fatigue limit and FCG threshold, as well as the notch tip radius ρ. Note that Eq. (25) predicts $q > 1$ for high $1/\kappa$ values, if the notch has a large tip radius ρ compared with the a_0 value, larger than a radius ρ_{sup} given by

$$\frac{\Delta S_{L0}\sqrt{\rho_{\sup}}}{\Delta K_{th0}} > \frac{1+q_0(\gamma)}{q_1(\gamma)} \Rightarrow \rho_{\sup} > \left(\frac{1+q_0(\gamma)}{q_1(\gamma)} \cdot \frac{\Delta K_{th0}}{\Delta S_{L0}}\right)^2. \tag{26}$$

Equation (26) is written for pulsating loads ($R = 0$), but it can be easily generalized for any other R ratio. It may seem strange to predict a notch sensitivity $q > 1$ (as for fatigue design and similar applications $q = 1$ must be used in such cases because by definition $K_f \leq K_t$), but such values have a good physical interpretation: sensitivities $q > 1$ mean that the cracks initiated by fatigue under fixed load conditions $\{\Delta\sigma, \sigma_{max}\}$ from the notch border do not stop, thus never become non-propagating under such conditions. This occurs when the stress gradient near the notch tip is too gentle to affect the short crack behaviour. In fact, in the absence of compressive residual stresses, the only mechanical reason for cracks induced by fatigue from a notch border to stop after growing for a while (under the same fixed load conditions that initiated them) inside an isotropic material is the stress gradient near the notch tip. To stop a crack, the stress range decrease ahead of the notch tip induced by the stress gradient around it must be able to surpass the SIF increase induced by the crack size increment, in such a way that $\Delta K = \eta \cdot \varphi(a) \cdot \Delta\sigma\sqrt{(\pi a)}$ can decrease as a grows until becoming smaller than the propagation threshold $\Delta K_{th0}(a)$ (or $\Delta K_{thR}(a)$ for $R \neq 0$). The crack stop size a_{st} (under pulsating loads) is thus reached when

$$\begin{aligned}\Delta K_I &= \eta \cdot \varphi(a_{st}) \cdot \Delta\sigma\sqrt{\pi a_{st}} = \Delta K_{th0}(a) \\ &= \Delta K_{th0} \cdot \left[1 + (a_0/a_{st})^{\gamma/2}\right]^{-1/\gamma}.\end{aligned} \tag{27}$$

Equation (25) can also possibly predict $q < 0$, that is, negative notch sensitivities (up to $q \cong -0.2$ in the Kirsch hole case, see Fig. 7), which seems even more strange than the $q > 1$ values. This occurs when the notch is too sharp, with a tip radius ρ_{inf} given by

$$\begin{aligned}&\Delta S_{L0}\sqrt{\rho_{\inf}}/\Delta K_{th0} < q_0(\gamma)/q_1(\gamma) \Rightarrow \\ &\rho_{\inf} < \left[\left(q_0(\gamma)\right)/q_1(\gamma) \cdot (\Delta K_{th0}/\Delta S_{L0})\right]^2.\end{aligned} \tag{28}$$

However, values $q < 0$ also have a clear physical interpretation: in such cases, it is easier to start a fatigue crack from a notchless surface than from the notch border. This occurs because the stress gradient $\partial g(a)/\partial a$ near the notch tip is so large that the SIF of the crack quickly reaches the long crack condition limit, which does not include any more the free surface factor $\eta = 1.12$, which affects the SIF of the cracks that start from unnotched surfaces. In most materials, the value of ρ_{inf} is on the order of a few micrometres,[36] meaning that small internal defects with radii $\rho < \rho_{inf}$ are not harmful, hence that the cracks will start, as usual, at the free surface of the piece.

Traditional semi-empirical notch sensitivity estimates, such as Peterson's $q = (1 + \alpha/\rho)^{-1}$, based on an ill-defined length parameter α obtained by fitting only seven experimental points, suppose that the notch sensitivity depends only on the notch tip radius ρ and on the steel tensile strength S_U, and only on ρ for Al alloys. The model proposed here, on the other hand, recognizes that q depends on ρ, ΔS_{L0}, ΔK_{th0}, γ, and also on the component and notch geometries, which affect the stress gradient ahead of the notch tip. There are reasonable relations between ΔS_{L0} and S_U, but none between ΔK_{th0} and S_U. This means that two steels of the same S_U, but very different ΔK_{th0}, should behave identically according to Peterson-like q estimates, whereas they usually do not. To quantify such evaluations, 450 steels and Al alloys with reported S_U, $S_L(R = -1)$ and ΔK_{th0} values were gathered in VIDA's database.[25,26,37] The steels set was separated in 400, 800,

1200, 1600 and 2000 MPa strength ranges, to use their average fatigue limits and FCG thresholds in the notch sensitivity analyses. All Al alloys were analysed with respect to their average strength $S_U = 225$ MPa. Assuming $R = -1$, their average fatigue limits were used to calculate a_0. The values so obtained were used to produce $q \times \rho$ curves for the Kirsch hole (Fig. 8), assuming a typical value $\gamma = 6$. Note how such curves reproduce quite well the curves proposed by Peterson a long time ago.[32]

Notch sensitivities for semi-elliptical notches in Al alloys, estimated using their average fatigue properties mentioned previously, are shown in Fig. 9. They depend on ρ, $\Delta S_L(R = -1) \cong S_L$, ΔK_{th0}, γ and also on their c/b ratios. Thus, they depend also on the notch shape, not only

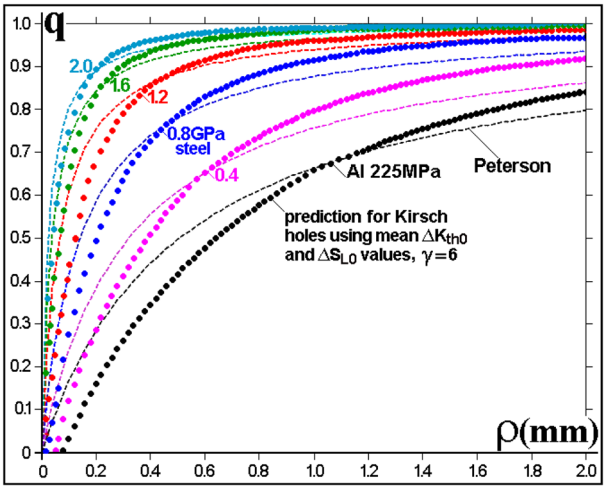

Fig. 8 Notch sensitivity q for Kirsch holes, estimated using mean ΔK_{th0} and ΔS_{L0} values from 450 steels and Al alloys, supposing $\gamma = 6$. Note that $q = 0$ means that it is easier to initiate a crack from a free surface than from the border of very small holes.

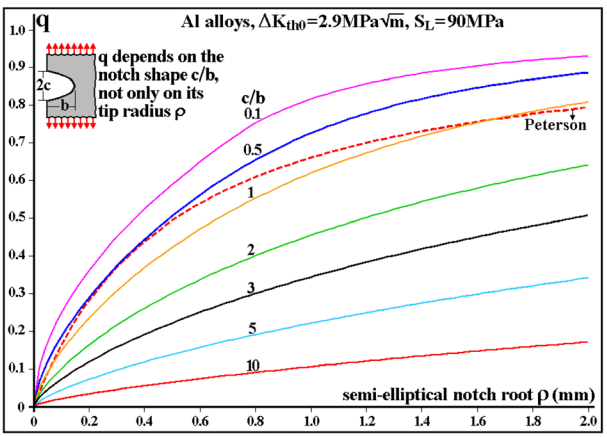

Fig. 9 Notch sensitivity q as a function of the tip radius ρ of semi-elliptical notches in Al alloys, estimated using $a_0 = (1/\pi)(\Delta K_{th0}/1.12S_{L0})^2 = 264\,\mu$m, $S_U = 225$ MPa and $\gamma = 6$.

on their tip radii ρ, as assumed in traditional SN analyses. As a matter of fact, they slightly depend on the R ratio as well, because it affects a little bit the $\Delta K_{thR}/S_{LR}$ ratio. Because the c/b ratio effect is very significant, it cannot be ignored in practice. The notch sensitivity of steels can be calculated in the same way, and it follows a similar pattern. Therefore, the observations made earlier for the parameters that control q in Al alloys are valid for steels as well. Further details on such calculations can be found in Ref. [25].

A different approach to model the notch sensitivity problem, called the theory of critical distances (TCD), is explored elsewhere.[38–41] Predictions made by the TCD model are similar but not identical to the predictions obtained by the stress gradient model proposed here. The TCD generalizes Peterson's and Neuber's original ideas, but the authors believe the stress gradient model is based on clearer mechanical bases and is easier to apply to notched components. The effect of microstructural defects on fatigue strength is deeply studied by Murakami.[36]

EXPERIMENTAL VERIFICATION OF THE NOTCH SENSITIVITY PREDICTIONS ON FATIGUE

Stop holes are widely used as an emergency crack repair technique. The hole is drilled at the crack front to remove its tip and to force it to re-initiate before restating its growth process. This simple trick may increase the cracked component durability, but its efficiency depends on several variables, among them the stop-hole radius ρ. To quantify how beneficial such holes can be, 23 precracked SE(T) test specimens with width $w = 80$ mm and thickness $t = 8$ mm (Fig. 10) were repaired in this way and then fatigue tested under constant force amplitudes at $R = 0.57$.[42] They were all cut from a plate of a 6082 T6 Al alloy (0.7–1.3Si, 0.6–1.2Mg, 0.4–1.0Mn, 0.5Fe, 0.25Cr, 0.2Zn, 0.1Cu and 0.1Ti) with yield strength $S_Y = 280$ MPa, $S_U = 327$ MPa, Young's modulus $E = 68$ GPa, reduction in area $RA = 12\%$ and Vickers hardness $HV_{50} = 95$ kg/mm^2, in its Longitudinal-Transversal (LT) direction. This alloy is used, for example, in vehicles, railway components and shipbuilding.

The fatigue tests were all performed at 30 Hz on a 100 kN computer controlled servo-hydraulic machine, following ASTM E647 procedures. The high $R = 0.57$ was chosen to avoid crack closure effects. After precracking a specimen, a stop hole with radius $\rho = 1$, 2.5, or 3 mm was carefully centred and drilled at its crack tip. To do so, the cracked specimens were removed from the testing machine, fixed on a milling machine, drilled at low feedings with plenty refrigeration and then finally reamed to generate elongated notches with a tip diameter accuracy of 1.5 µm, all with the same initial size

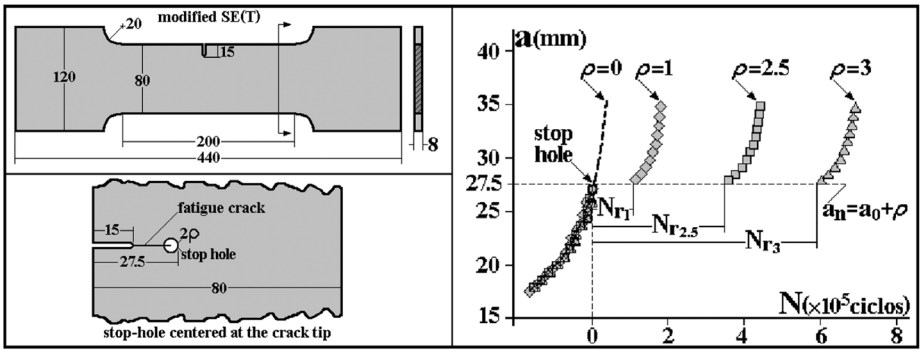

Fig. 10 Test specimen used to test the stop-hole size effect on their efficiency as a crack repair method and typical results obtained with them.

$a_i = 27.5\ \text{mm} \Rightarrow a_i/w = 0.344$, to avoid interference of possible crack length or residual ligament $rl = w - a_i$ effects. Great care was taken to avoid introducing residual stresses around the stop hole by any means during its drilling and reaming process. Finally, the test specimens were remounted on the test machine, and the fatigue test was restarted under the previous loading conditions. Figure 11 also shows typical data obtained from such repaired specimens. Table 1 summarizes the testing conditions after introducing the stop holes, and the fatigue life increments obtained from them. The pseudo SIFs of the repaired specimens listed in this table, $\Delta K^* = 1.895\ \Delta P/t\sqrt{w}$, were calculated using the SIF expression for the SE(T) with identical a/w, given by[43]

The fatigue crack re-initiation lives at the stop-hole tips can be reliably modelled by traditional εN procedures. This modelling process requires the cyclic properties of the 6082 T6 Al alloy, that is, Ramberg–Osgood's $k' = 443$MPa and $n' = 0.064$ and Coffin–Manson's $\sigma_f' = 485$ MPa, $b = -0.0695$, $\varepsilon_f' = 0.733$ and $c = -0.827$;[44] the nominal stress history (Table 1); and the SCF of the notches generated by the stop holes. These can be estimated by Creager and Paris,[45] giving, for example, $K_t \cong 12.38$ for a stop hole with radius $\rho = 1$, or else by Inglis,[46] $K_t \cong 1 + 2\sqrt{(a/\rho)} = 11.49$ in this case; but the resulting notch SCFs were instead calculated by finite elements: $K_t = 11.8$, 8.1 and 7.6 for $\rho = 2.5$

$$K_I = \frac{P}{t\sqrt{w}}\left(1.99\left[\frac{a}{w}\right]^{0.5} - 0.41\left[\frac{a}{w}\right]^{1.5} + 18.7\left[\frac{a}{w}\right]^{2.5} - 38.85\left[\frac{a}{w}\right]^{3.5} + 53.85\left[\frac{a}{w}\right]^{4.5}\right). \quad (29)$$

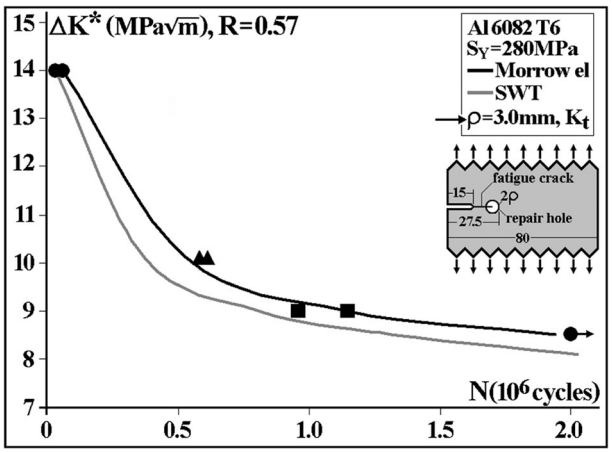

Fig. 11 Fatigue crack re-initiation lives measured for the larger stop-holes with tip radius $\rho = 3.0$ mm and fatigue lives predicted by εN procedures using the resulting elongated notch stress concentration factor K_t calculated by FE in Neuber's rule (ΔK^* is the pseudo-stress intensity factor applied on the notch).

and 3 mm, respectively. The life improvement induced by the stop holes can be estimated by calculating stresses and strains at their borders by Neuber's rule, and then the crack re-initiation lives considering mean load effects. Such effects cannot be neglected, because the R ratio used in the tests was high. In fact, Coffin-Manson predictions are highly non-conservative, thus useless in this case. Figures 11–14 show that the lives predicted by Morrow EL and by Smith–Watson–Topper (SWT) are similar in this case (but such a similarity cannot be assumed beforehand; because in many other cases, these rules can predict very different fatigue lives).[26]

The lives predicted using K_t for the two larger stop-holes reproduced reasonably well the tests results, see Fig. 11 for the $\rho = 3$ mm results. However, the lives predicted using K_t for the $\rho = 1$ mm stop hole shown in Fig. 12 are too conservative in comparison with the measured data. Such better-than-predicted fatigue lives of course do not mean that the smaller hole is more efficient

Table 1 Crack re-initiation lives N_r after introducing the stop hole at their tips

$\rho = 1$ mm		$\rho = 2.5$ mm		$\rho = 3$ mm	
ΔK^*MPa$\sqrt{m}$	$N_r \times 10^3$ cycles	ΔK^*MPa$\sqrt{m}$	$N_r \times 10^3$ cycles	ΔK^*MPa$\sqrt{m}$	$N_r \times 10^3$ cycles
6.0	>2000	7.5	>2000	8.5	>2000
7.4	980, 724, 580	8.1	1800	9.0	1150, 960
8.0	600, 560, 510	10.1	355, 270	10.1	611, 580
10.1	119, 84	13.5	65, 58, 37	14.0	60, 32

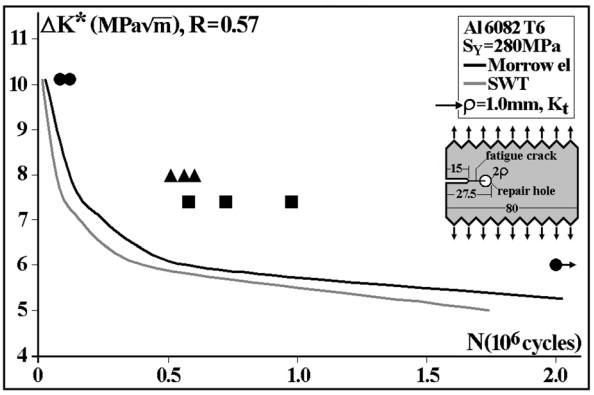

Fig. 12 Similar to Fig. 11, but for the smaller stop-holes with tip radius $\rho = 1.0$ mm.

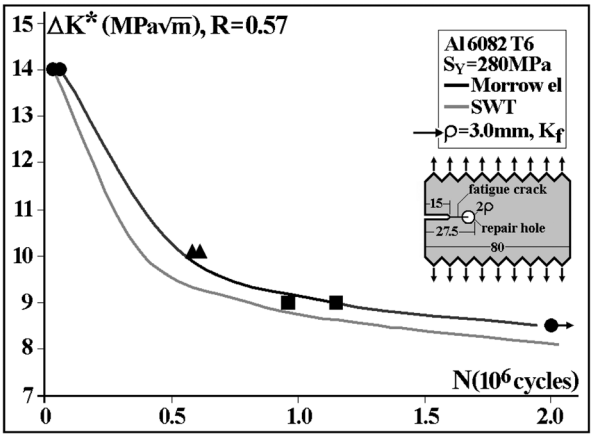

Fig. 13 Fatigue crack re-initiation lives measured for the stop-hole root with radius $\rho = 3.0$ mm and predicted using the resulting elongated notch fatigue stress concentration factor K_f calculated by the procedures proposed in this paper in Neuber's rule (ΔK^* is the pseudo-stress intensity factor applied on the notch).

than the larger ones, as the larger stop-holes are associated with longer fatigue crack re-initiation lives for a given load, see Table 1. Therefore, from a modeling point of view, the main result obtained from such figures is that εN life predictions made using traditional procedures based on K_t, Neuber, and Morrow or Smith–Watson–Topper were satisfactory for the larger

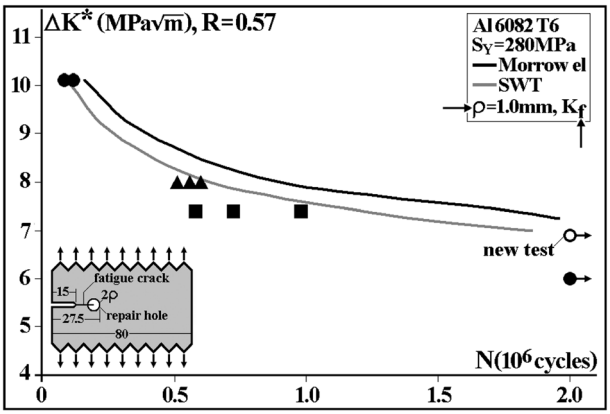

Fig. 14 Similar to Fig. 13, but for the smaller stop-holes with tip radius $\rho = 1.0$ mm and $K_f < K_t$.

stop-holes, but severely underestimated the re-initiation lives for the smaller ones.

The better-than-expected fatigue lives obtained from the smaller stop-holes could be due to compressive residual stresses. However, all stop holes were drilled and reamed following identical procedures, and their diameters were all large enough to remove the previous crack tip plastic zones, leaving only virgin material ahead of their tips. Hence, because the larger stop-hole lives were well predicted, supposing $\sigma_{res} = 0$, it is difficult to justify why high compressive residual stresses would be present only around the smaller stop-hole tips. The same can be said about the stop holes' surface finish. However, the smaller stop-holes generate larger SCF than the larger ones; therefore, they induce a steeper stress gradient ahead of their tips. This effect can significantly affect the growth of short cracks and, consequently, the fatigue notch sensitivity of the stop hole. Indeed, when using the properly calculated fatigue SCF K_f instead of K_t with the traditional εN procedures, considering the elongated notch sensitivity q by the method proposed here, all estimated fatigue crack re-initiation lives reproduce quite well the measured results (Figs 13 and 14). The Al 6082 T6 fatigue limit and fatigue crack propagation threshold under pulsating loads ($R = 0$) needed to calculate K_f are estimated as $\Delta K_{tb0} = 4.8$ MPa$\sqrt{m}$ and

$\Delta S_{L0} = 110$ MPa, following traditional structural design practices, and $\gamma = 6$.

Note that the K_t-based predictions shown in Fig. 11 are very similar to the K_f-based predictions shown in Fig. 13, because the larger stop-holes have $q \cong 1$. However, the K_f-based life predictions for the smaller $\rho = 1$ mm stop-holes shown in Fig. 14 are much better than the K_t-based predictions shown in Fig. 12. Note also that the word *prediction* can in fact be used here, because the curves shown in such figures result from fatigue crack re-initiation life estimates made using only mechanical principles and material data obtained from the literature, without considering any of the measured data points. Hence, they are really predicted, not data-fitted curves. Moreover, an additional test made after those calculations confirmed the prediction that the $\rho = 1$ mm stop-hole could tolerate a higher pseudo-SIF range $\Delta K^* = 7\text{MPa}\sqrt{\text{m}}$, as indeed it did (Fig. 14).

NOTCH SENSITIVITY EFFECTS ON ENVIRONMENTALLY ASSISTED CRACKING

Environmentally assisted cracking involves the nucleation and/or propagation of cracks in susceptible materials immerged in aggressive media. This time-dependent chemical/mechanical damage mechanism may eventually lead to fracture under static tensile stresses that might be well below the material strength in benign environments. EAC mechanisms are usually subdivided into the following sub-mechanisms: SCC, due to chemical reactions at crack tips enhanced by the high stresses that surround them; hydrogen embrittlement, due to high hydrostatic stresses induced by penetration of small H atoms inside the gaps of crystalline lattices and/or grain boundaries; liquid metal embrittlement (LME), due to the interaction of liquid metals such as Hg, Pb, Ga, Cd or Zn with tensioned surfaces of LME-sensitive structural alloys; solid metal embrittlement in tensioned coatings or inclusions; and corrosion fatigue, due to a synergic interaction between cyclic loads and electrochemical reactions at crack tips. Such EAC mechanisms may have different phenomenologies, but they all have a common feature: unlike other corrosion problems, they depend both on the environment/material pair and on the stress state, because cracks cannot grow unless loaded by tensile stresses. Hence, all EAC mechanisms require an EAC-sensitive material, an aggressive medium and tensile stresses.[47–58]

Indeed, cracks only grow if driven by tensile stresses, and the environment contribution is to decrease the material resistance to the cracking process. As the terminology *stress corrosion cracking* enhances this mutual dependence, it is preferred here to name all EAC mechanisms as SCC when there is no need separate them. Such problems are important for many industries, because costs and delivery times for special SCC-resistant alloys are large and keep increasing. Major SCC problems occur, for example, in the oil industry, because oil and gas fields can contain considerable amounts of H_2S, which may attack steel pipelines, and in the aeronautical industry, when their light aluminum structures must operate in saline environments, such as in aircraft carriers, offshore platforms or coastal airports.

However, for structural analysis purposes, most SCC problems have been treated so far by a simplistic overconservative policy on susceptible material-environment pairs: if aggressive media are unavoidable during the service lives of structural components, the standard design solution is to choose a material resistant to SCC in such media to build them. A less expensive alternative solution may be to recover the structural component surface with a suitable nobler coating, if such a coating is available. SCC-proof coatings must be properly adherent, scratch resistant and more reliable than common corrosion-resistant coatings, because structural components can fail without warning under such conditions. Such overconservative design criteria may be safe, but they can also be too expensive if an otherwise attractive material is summarily disqualified in the design stage when it may suffer SCC in the service environment, without considering any stress analysis issues. Nevertheless, the SCC behaviour cannot be properly evaluated neglecting the influence of the stress fields that drive them. Decisions based on such an inflexible pass/fail approach may cause severe cost penalties, because no crack can grow unless driven by a tensile stress caused by the service loads and by the residual stresses induced by previous loads and overloads.

In other words, although EAC conditions may be difficult to define in practice due to the number of metallurgical, chemical and mechanical variables that may affect them, sound structural integrity assessment procedures must include proper stress analysis techniques for calculating maximum tolerable flaw sizes. Such techniques are important in the design stage, but they are even more useful to evaluate operating structural components not originally designed for SCC service, when by any reason they must begin to work under such conditions due to some unavoidable operational change (e.g. a pipeline that must transport originally unforeseen amounts of H_2S due to changes in oil well conditions while a new one specifically designed for such service is built and commissioned.) Economical pressures to take such a structural risk may be inescapable, because loss of profits associated with the very long time required for replacing the component can be huge, especially in offshore applications. Such risky decisions can in principle be controlled by the methodology proposed as follows, which extends to EAC problems the analysis developed to mechanically quantify notch sensitivity effects through the behaviour of short fatigue cracks.

Indeed, if cracks behave well under SCC conditions, that is, if fracture mechanics concepts can be used to describe them, then a 'short crack characteristic size under SCC conditions' can be defined by[59]

$$a_{0_{SCC}} = (1/\pi)\cdot[K_{ISCC}/(\eta\cdot S_{SCC})]^2. \qquad (30)$$

In this way, if all chemical effects involved in SCC problems can be as usual assumed to be properly described and quantified by the traditional material resistances to crack initiation and propagation in the service medium under fixed stress conditions, S_{SCC} and K_{ISCC}, supposing such pairs remain fixed, the a_0 concept in SCC follows exactly the same idea of its analogous short crack characteristic size so useful for fatigue purposes: it matches the otherwise separated material resistances K_{ISCC} and S_{SCC} to describe the behaviour of mechanically short cracks and as so can potentially be equally useful in SCC problems. Such resistances are well-defined material properties for a given environment and can be measured by standard procedures. Moreover, although SCC problems are time dependent, S_{SCC} and K_{ISCC} are not, because they quantify the limit stresses required for starting or for growing cracks under SCC conditions. Hence, supposing that the mechanical parameters that limit SCC damage behave analogously to the equivalent parameters ΔK_{tbR} and ΔS_{LR} that limit fatigue damage, a Kitagawa-like diagram can be used to quantify the crack sizes a tolerable by any given component that works in SCC conditions under a given tensile stress σ, see Fig. 15.

This idea makes sense as well if K_{ISCC} and S_{SCC} are viewed as the limits as $R \to 1$ for ΔK_{tbR} and ΔS_{LR} in the given medium and can be further expanded. For example, Fig. 16 presents an extended Kitagawa–Takahashi diagram that shows four regions that may contain non-propagating cracks. First, starting from the bottom, the region bounded by the material resistances to crack initiation and large crack growth by fatigue in a given aggressive

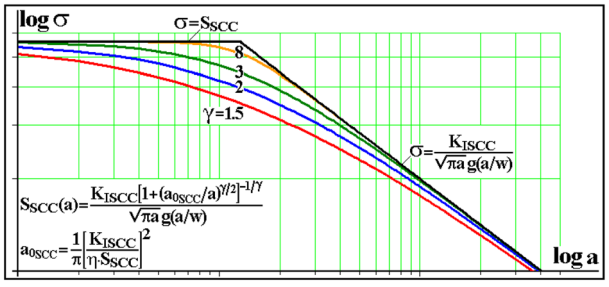

Fig. 15 A Kitagawa–Takahashi-like diagram proposed to describe the environmentally assisted cracking behaviour of short and deep flaws for structural design purposes.

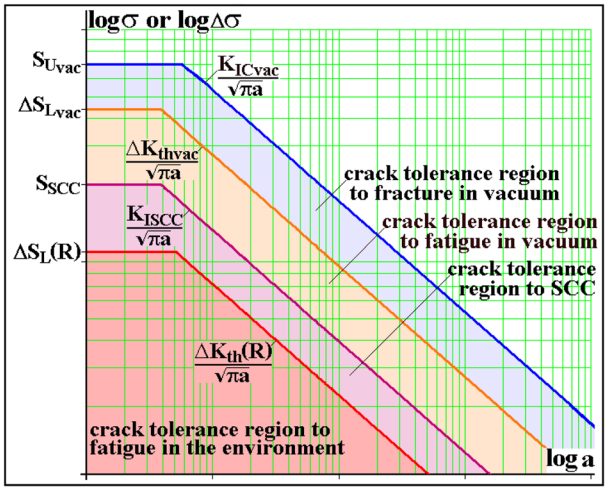

Fig. 16 Extended Kitagawa diagram including fatigue and stress corrosion cracking limiting conditions for crack growth.

medium ΔS_{LR} and $\Delta K_{tbR}/\sqrt{(\pi a)}$, which limits the tolerance zone that may contain non-propagating fatigue cracks in that environment under fixed range loads at a given R ratio; second, the region limited by S_{SCC} and $K_{ISCC}/\sqrt{(\pi a)}$ that may contain non-propagating cracks by SCC in that medium; third, the crack tolerance region limited by ΔS_{Lvac} and ΔK_{tbvac}, the R-independent fatigue limit and FCG threshold of the given material in vacuum; and fourth, the region limited by the intrinsic material properties S_{Uvac} and $K_{ICvac}/\sqrt{(\pi a)}$, which can only be measured in vacuum or in truly inert environments. The main advantage of looking at this problem in such an integrated way is that it turns natural the attempt to treat mechanical and chemical damage under a unified analysis procedure, following, for example, Vasudevan and Sadananda's Unified Approach methodologies.[60,61]

In other words, if cracks loaded under SCC conditions behave as they should, that is, if their mechanical driving force is indeed the SIF applied on them; and if the chemical effects that influence their behaviour are completely described by the material resistance to crack initiation from smooth surfaces quantified by S_{SCC} and by its resistance to crack propagation measured by K_{ISCC}; then, it can be expected that cracks induced by SCC may depart from sharp notches and then stop, due to the stress gradient ahead of the notch tips, eventually becoming non-propagating cracks, exactly as in the fatigue case. In such cases, the size of non-propagating short cracks can be calculated using the same procedures used for fatigue, and the tolerance to such defects can be properly quantified using an SCC notch sensitivity factor in structural integrity assessments. Hence, a criterion for the maximum tolerable stress under SCC conditions can be proposed as follows:

$$\sigma_{max} \leq K_{ISCC} / \left\{ \sqrt{\pi a} \cdot g(a/w) \cdot \left[1. + (a_{0_{SCC}}/a)^{\gamma/2} \right]^{1/\gamma} \right\}, \quad (31)$$
$$a_{0_{SCC}} = (1/\pi)[K_{ISCC}/(\eta \cdot S_{SCC})]^2$$

In the same way, an expression analogous to Eq. (25) can be used to properly define a 'notch sensitivity under EAC conditions' by solving for a given γ (if it is necessary to better fit the data) the system $\{\varphi/g = 1,\ \partial(\varphi/g)\partial x = 0\}$ for several notch tip radii ρ using $\kappa \equiv K_{ISCC}/(S_{SCC}\sqrt{\rho})$ to obtain

$$q_{SCC}(\kappa, \gamma) \equiv [K_{t_{SCC}}(\kappa, \gamma) - 1]/(K_t - 1) \quad (32)$$

where q_{SCC} and $K_{tSCC} = 1 + q_{SCC}(K_t - 1)$ are the notch sensitivity and the effective SCF under EAC conditions. In this way, q_{SCC} and K_{tSCC} can be seen as analogous to the q and K_f parameters used for stress analyses under fatigue conditions.

Such equations can be used for stress analyses of notched components under SCC conditions. Hence, they are potentially useful for structural design purposes when overconservative pass/non-pass criteria used to 'solve' most practical SCC problems nowadays are not affordable or cannot be used for any other reason. In fact, they can form the basis for a *mechanical* criterion for SCC that can be applied even by structural engineers, because it does not require much expertise in chemistry to be useful. Moreover, they can be properly tested, as follows.

First, following expert advice (Vasudevan, private communication), the basic SCC resistances were measured for the Al 2024 – liquid gallium pair (Ga is liquid above 30 °C, but curiously it only boils at 2204 °C). The main advantage of this exotic material-environment pair is its very quick SCC (in fact, LME) reactions, in the order of minutes. In comparison, SCC-sensitive Al alloys may take weeks to crack in NaCl-water solutions. Moreover, contrary to other liquid metals that may cause LME such as mercury, Ga is a safe, non-toxic material.

This 2024 Al alloy was originally obtained in a T351 temper as a 12.7 mm thick plate, with analysed composition Al plus 4.44Cu, 1.35Mg, 0.54Mn, 0.18Zn, 0.16Fe, 0.12Si, 0.02Cr, 0.01Zr and less than 0.05 of other elements in weight percentage. However, the alloy had to be annealed to remove its residual stresses, because in the original as-received plate condition, the Ga environment would induce the test specimens to break during manipulation. All test specimens were cut on the Transversal-Longitudinal (TL) direction of the plate, identified by metallographic procedures. The basic mechanical properties of the annealed 2024 Al alloy were measured following ASTM E8M standard procedures at 35 °C, resulting in $E = 70$GPa, $S_Y = 113$ MPa, $S_U = 240$ MPa and ultimate strain $\varepsilon_U = 16\%$.

Stress corrosion cracking sensibility and reaction rates of the Al–Ga pair were qualitatively evaluated also at 35 °C in very slow $d\varepsilon/dt = 4.5 \times 10^{-8}$/s strain rate tension tests made in servo-controlled electromechanical testing machines, following ASTM G129 and the NACE International, the Corrosion Society recommendations. The liquefied Ga was applied on the test specimens surfaces with a brush, and light bulbs were used to maintain the warm 35 °C temperature during the tests (Fig. 17). To guarantee that the exposure time was long enough to ensure the LME phenomenon, the time necessary to propagate a crack in the annealed Al 2024 – liquid Ga pair was double-checked by testing precracked C(T) specimens such as those used to measure K_{ISCC}.

Two such specimens were tested under 7.5 MPa$\sqrt{\text{m}}$, and two others under 12 MPa$\sqrt{\text{m}}$. The latter failed in less than 3 h, whereas the others did not fail after 2 days. So, following standard procedures and assuming that the incubation time should be a value close to 3 h, a preload of 7.5 MPa$\sqrt{\text{m}}$ was applied for 1 day on the test specimens used for measuring K_{ISCC}. Similarly, a preload of 30 MPa was applied for 1 day on the test specimens used to measure S_{SCC}. Such basic SCC resistances were measured using incremental load steps induced by calibrated load rings following ASTM E1681, ASTM F1624 and ISO 7539 standard procedures: S_{SCC} tests started at 30 MPa and used 2.5 MPa steps and K_{ISCC} tests initiated at 7.5 MPa$\sqrt{\text{m}}$ and used 0.25 MPa$\sqrt{\text{m}}$ steps.

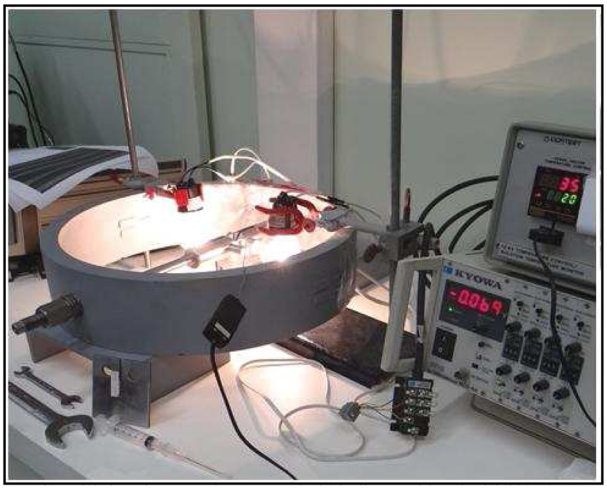

Fig. 17 Load ring and warming light bulbs used for the stress corrosion cracking tests.

Fig. 18 Initially smooth test specimen with 6.35mm diameter, used for measuring S_{SCC}, the resistance to crack initiation under SCC, according to ASTM F1624 and ISO 7539 standards.

The time between successive load steps was at least one hour. The measured values were $S_{SCC} = 43.6 \pm 4.2$ MPa (average of *nine* samples, with 95% reliability) and $K_{ISCC} = 8.8 \pm 0.3$ MPa$\sqrt{\text{m}}$ (*eight* samples, 95% reliability). Some of the test specimens broken during such standard SCC tests are shown in Figs 18 and 19.

Fig. 19 C(T) specimen with $w = 60$ *mm* used for measuring K_{ISCC}, the resistance to crack propagation under SCC, according to ASTM E1681, ASTM F1624, and ISO 7539 procedures.

Finally, using such standard SCC properties, four pairs of C(T)-like notched test specimens were *designed* to support a maximum local stress $\sigma \cong 90\,\text{MPa} > 2 \cdot S_{SCC}$ at their notch tips. The dimensions chosen for such notches were $\{b,\ \rho,\ b/w\} = \{20\,\text{mm},\ 0.5\,\text{mm},\ 0.33\}$, $\{12\,\text{mm},\ 0.5\,\text{mm},\ 0.2\}$, $\{20\,\text{mm},\ 0.2\,\text{mm},\ 0.33\}$, $\{40\,\text{mm},\ 4.5\,\text{mm},\ 0.67\}$, respectively for specimens TS1–TS2, TS3–TS4, TS5–TS6 and TS7–TS8, where b and ρ are the notch depth and tip radius, and w is the specimen width, with both b and w measured from the load line. The idea was, of course, to study their SCF/stress gradient combinations in order to assure tolerance to the short cracks that should start at the tips of their notches, because they were loaded well above S_{SCC}. The (different) loads applied on each one of such notched test specimens were maintained for at least 48 h.

Despite being submitted to a much longer exposure than that required to measure S_{SCC} and K_{ISCC} according to standard procedures, none of such notched specimens failed during the tests, exactly as predicted beforehand. A pair of notched test specimens is shown in Fig. 20. Figure 21 shows some of the unbroken notched test specimens after being loaded under a maximum local stress at the notch tip higher than twice the material resistance to crack initiation under SCC conditions, $\sigma_{max} > 2 \cdot S_{SCC}$, for a period 50 times longer than the one from the S_{SCC} measurement tests.

(a) (b)

Fig. 20 (a) One of the four pairs of notched C(T)-like specimens used for testing the stress corrosion cracking notch sensitivity predictions; and (b) metrological verification of the notch dimensions.

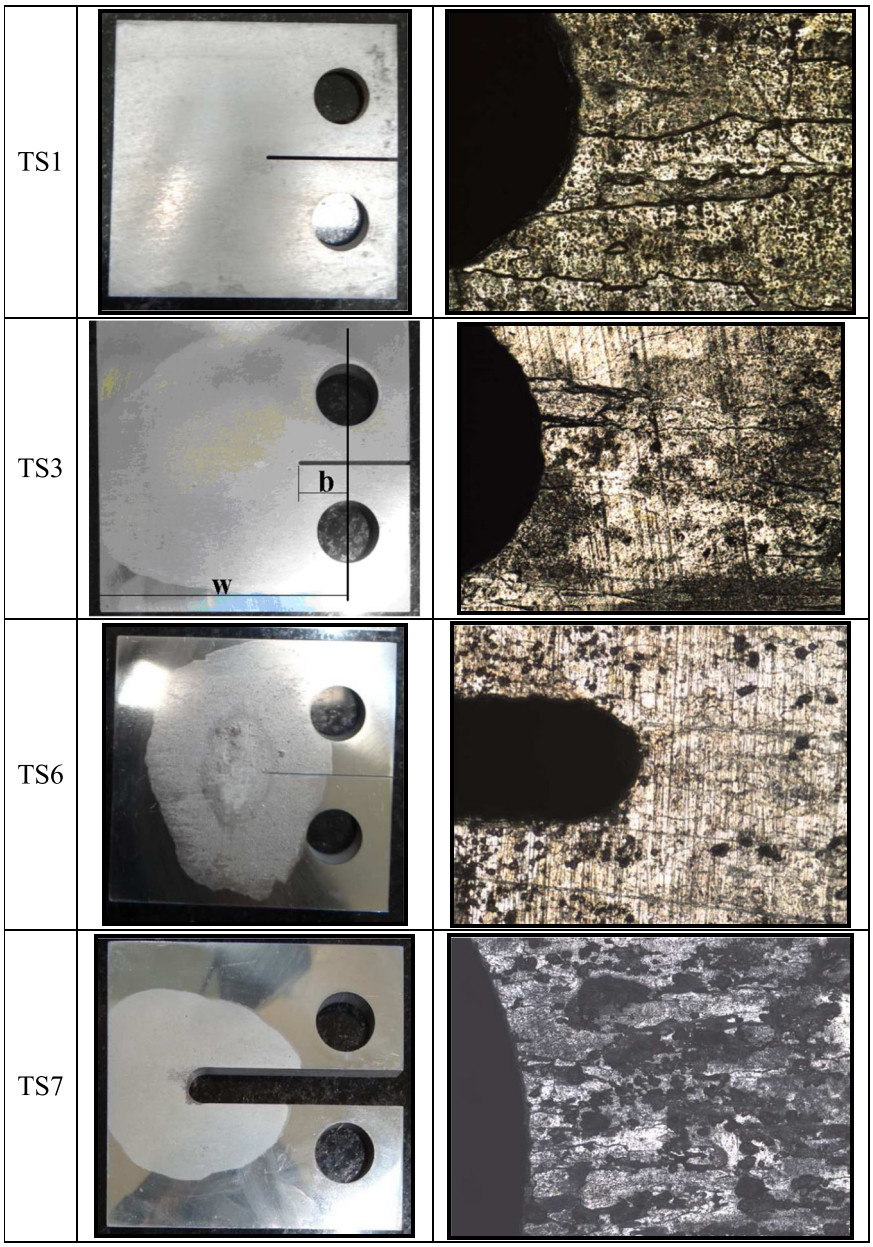

Fig. 21 Notched C(T)-like specimens, all with the same width $w = 60mm$ and, from top to bottom, with $\{b, r, b/w\} = \{20mm, 0.5mm, 0.33\}$, $\{12mm, 0.5mm, 0.2\}$, $\{20mm, 0.2mm, 0.33\}$, and $\{40mm, 4.5mm, 0.67\}$, after being tested under $S_{max} = 90MPa > 2{\times}S_{SCC}$ at the notch tip, or ***twice*** the stress that would lead unnotched specimens to fail by SCC.

CONCLUSIONS

A generalized ETS parameter was used to model the dependence of the threshold stress intensity range for short fatigue cracks on the crack size, as well as the behaviour of non-propagating cracks induced by EAC. This dependence was used to estimate the notch sensitivity factor q of shallow and of elongated notches both for fatigue and for EAC conditions, from studying the propagation behavior of short non-propagating cracks that might initiate from their tips. It was found that the notch sensitivity of elongated slits has a very strong dependence on the notch aspect ratio, defined by the ratio c/b of the semi-elliptical notch that approximates the slit shape having the same tip radius. These predictions were calculated by numerical routines and verified by proper experiments. On the basis of this promising performance, a criterion to evaluate the influence of small or large surface flaws in fatigue and in EAC problems was proposed. Such results indicate that notch sensitivity can indeed be properly treated as a mechanical problem.

Acknowledgements

CNPq, the Brazilian Research Council, and Petrobras, the Brazilian oil company, have provided research scholarships for some of the authors; Dr A. Vasudevan from ONR, the Office of Naval Research of the US Navy, has contributed with many stimulating discussions; and ONR has provided a grant to partially support this research.

REFERENCES

1 McEvily, A. J. (1988) The growth of short fatigue cracks: a review. *Mater. Sci. Res. Int.*, **4**, 3–11.
2 Sadananda, K. and Vasudevan, A. K. (1997) Short crack growth and internal stresses. *Int. J. Fatig.*, **19**, S99–S108.
3 Lawson, L., Chen, E. Y. and Meshii, M. (1999) Near-threshold fatigue: a review. *Int. J. Fatig.*, **21**, S15–S34.
4 Navarro, A. and de los Rios, E. R. (1988) A microstructurally-short fatigue crack growth equation. *Fatig. Fract. Eng. Mater. Struct.*, **11**, 383–396.
5 Chapetti, M. D. (2003) Fatigue propagation threshold of short cracks under constant amplitude loading. *Int. J. Fatig.*, **25**, 1319–1326.
6 Krupp, U., Düber, O., Christ, H. J., Künkler, B., Schick, A. and Fritzen, C. P. (2004) Application of the EBSD technique to describe the initiation and growth behaviour of microstructurally short fatigue cracks in a duplex steel. *J. Microsc.*, **213**, 313–320.
7 Chapetti, M. D. (2008) Fatigue assessment using an integrated threshold curve method – applications. *Eng. Fract. Mech.*, **75**, 1854–1863.
8 Verreman, Y. (2008) Propagation des fissures curtes. In: *Fatigue des Matériaux et Structures*, vol. **2** (Edited by C. Bathias and A. Pineau), Hermes-Lavoisier, Cachan, France.
9 Lorenzino, P. and Navarro, A. (2013) Initiation and growth behaviour of very-long microstucturally short fatigue cracks. *Frattura ed Integrità Strutturale*, **25**, 138–144.
10 El Haddad, M. H., Topper, T. H. and Smith, K. N. (1979) Prediction of non-propagating cracks. *Eng. Fract. Mech.*, **11**, 573–584.
11 El Haddad, M. H., Smith, K. N. and Topper, T. H. (1979) Fatigue crack propagation of short cracks. *J. Eng. Mater. Tech.*, **101**, 42–46.
12 Yu, M. T., Duquesnay, D. L. and Topper, T. H. (1988) Notch fatigue behavior of 1045 steel. *Int. J. Fatig.*, **10**, 109–116.
13 Kitagawa, H. and Takahashi, S. (1976) Applicability of fracture mechanics to very small crack or cracks in the early stage. *Second Int Conf Mech Behavior of Mat*, Boston, MA, 627–631, ASM.
14 Forman, R. G., Shivakumar, V., Mettu, S. R. and Newman, J. C. (2000) Fatigue crack growth computer program NASGRO version 3.0, Reference Manual, NASA.
15 Bazant, Z. P. (1997) Scaling of quasibrittle fracture: asymptotic analysis. *Int. J. Fract.*, **83**, 19–40.
16 Tanaka, K., Nakai, Y. and Yamashita, M. (1981) Fatigue growth threshold of small cracks. *Int. J. Fract.*, **17**, 519–533.
17 Livieri, P. and Tovo, R. (2004) Fatigue limit evaluation of notches, small cracks and defects: an engineering approach. *Fatig. Fract. Eng. Mater. Struct.*, **27**, 1037–1049.
18 Du Quesnay, D. L., Yu, M. T. and Topper, T. H. (1988) An analysis of notch-size effects at the fatigue limit. *J. Test. Eval.*, **16**, 375–385.
19 Vallellano, C., Navarro, A. and Dominguez, J. (2000) Fatigue crack growth threshold conditions at notches. Part I: theory. *Fatig. Fract. Eng. Mater. Struct.*, **23**, 113–121.
20 Atzori, B., Lazzarin, P. and Filippi, S. (2001) Cracks and notches: analogies and differences of the relevant stress distributions and practical consequences in fatigue limit predictions. *Int. J. Fatig.*, **23**, 355–362.
21 Atzori, B., Lazzarin, P. and Meneghetti, G. (2003) Fracture mechanics and notch sensitivity. *Fatig. Fract. Eng. Mater. Struct.*, **26**, 257–267.
22 Ciavarella, M. and Meneghetti, G. (2004) On fatigue limit in the presence of notches: classical vs. recent unified formulations. *Int. J. Fatig.*, **26**, 289–298.
23 Atzori, B., Meneghetti, G. and Susmel, L. (2005) Material fatigue properties for assessing mechanical components weakened by notches and defects. *Fatig. Fract. Eng. Mater. Struct.*, **28**, 83–97.
24 Atzori, B., Lazzarin, P. and Meneghetti, G. (2005) A unified treatment of the mode I fatigue limit of components containing notches or defects. *Int. J. Fract.*, **133**, 61–87.
25 Meggiolaro, M. A., Miranda, A. C. O. and Castro, J. T. P. (2007) Short crack threshold estimates to predict notch sensitivity factors in fatigue. *Int. J. Fatig.*, **29**, 2022–2031.
26 Castro, J. T. P., Meggiolaro, M. A., Miranda, A. C. O., Wu, H., Imad, A. and Nouredine, B. (2012) Prediction of fatigue crack initiation lives at elongated notch roots using short crack concepts. *Int. J. Fatig.*, **42**, 172–182.
27 Barsom, J. M. and Rolfe, S. T. (1999) *Fracture and Fatigue Control in Structures*, 3rd edn. ASTM, West Conshohocken, PA, USA.
28 Newman, J. C. and Raju, I. (1984) Stress-intensity factor equations for cracks in three-dimensional finite bodies subjected to tension and bending loads, NASA TM-85793.
29 Góes, R. C. O., Castro, J. T. P. and Martha, L. F. (2013) 3D effects around notch and crack tips. *Int. J. Fatig.*, doi: 10.1016/j.ijfatigue.
30 Castro, J. T. P. and Leite, J. C. C. (2013) Does notch sensibility exist in environmentally assisted cracking (EAC)? *J. Mater. Res. Tech.*, **2**, 288–295.
31 Schijve, J. (2001) *Fatigue of Structures and Materials*. Kluwer, Dordrecht, Netherlands.
32 Peterson, R. E. (1974) *Stress Concentration Factors*. Wiley, Hoboken, NJ, USA.
33 Frost, N. E., Marsh, K. J. and Pook, L. P. (1999) *Metal Fatigue*. Dover, Mineola, NY, USA.
34 Tada, H., Paris, P. C. and Irwin, G. R. (1985) *The Stress Analysis of Cracks Handbook*. Del Research, St. Louis, Mo, USA.
35 Miranda, A. C. O., Meggiolaro, M. A., Martha, L. F. and Castro, J. T. P. (2012) Stress intensity factor predictions: comparison and round-off error. *Comput. Mater. Sci.*, **53**, 354–358.
36 Murakami, Y. (2002) *Metal Fatigue: Effects of Small Defects and Non-Metallic Inclusions*. Elsevier, Amsterdam, Netherlands.
37 Meggiolaro, M. A. and Castro, J. T. P. (2010) Automation of the fatigue design under variable amplitude loading using the ViDa software. *Int. J. Struct. Integrity*, **1**, 94–103.
38 Taylor, D. (1999) Geometrical effects in fatigue: a unifying theoretical model. *Int. J. Fatig.*, **21**, 413–420.
39 Taylor, D. (2007) *The Theory of Critical Distances*. Elsevier.
40 Susmel, L. (2008) The theory of critical distances: a review of its applications in fatigue. *Eng. Fract. Mech.*, **75**, 1706–1724.
41 Susmel, L. and Taylor, D. (2010) The Theory of Critical Distances as an alternative experimental strategy for the determination of K_{IC} and ΔK_{th}. *Eng. Fract. Mech.*, **77**, 1492–1501.
42 Wu, H., Imad, A., Nouredine, B., Castro, J. T. P. and Meggiolaro, M. A. (2010) On the prediction of the residual fatigue life of cracked structures repaired by the stop-hole method. *Int. J. Fatig.*, **32**, 670–677.

43 Rabbe, P., Lieurade, H. P. and Galtier, A. (2000) *Essais de fatigue*, *partie I*. Techniques de l'Ingénieur, Traité M4170. www.techniques-ingenieur.fr. (accessed on 16/01/2013).
44 Borrego, L. P., Ferreira, J. M., Pinho da Cruz, J. M. and Costa, J. M. (2003) Evaluation of overload effects on fatigue crack growth and closure. *Eng. Fract. Mech.*, **70**, 1379–1397.
45 Creager, M. and Paris, P. C. (1967) Elastic field equations for blunt cracks with reference to stress corrosion cracking. *Int. J. Fract. Mech.*, **3**, 247–252.
46 Inglis, C. E. (1913) Stress in a plate due to the presence of cracks and sharp corners. *Phil. Trans. Roy. Soc. A*, **215**, 119–233.
47 McEvily, A. J. and Wei, R. P. (1972) *Corrosion Fatigue – Chemistry, Mechanics & Microstructure*, vol. **2**. NACE, Huston, TX, USA, pp. 381–395.
48 Fontana, M. G. (1986) *Corrosion Engineering*. McGraw Hill, New York, NY, USA.
49 *Corrosion*, ASM Handbook, ASM, Materials Park, OH, USA, vol. **13**. (1992).
50 Leis, B. N. and Eiber, R. J. (1997) Stress-corrosion cracking on gas-transmission pipelines: history, causes, and mitigation. *First Int Business Conf Onshore Pipelines*, Berlin, Germany.
51 Dietzel, W. (2001) Fracture mechanics approach to stress corrosion cracking. *Anales de Mecánica de la Fractura*, **18**, 1–7.
52 Lynch, S. P. (2003) Failures of engineering components due to environmentally assisted cracking. *Pract. Fail. Anal.*, **3**, 33–42.
53 *Corrosion: Fundamentals, Testing, and Protection*, ASM Handbook, ASM, Materials Park, OH, USA, vol. **13A**. doi: 10.1016/j.ijfatigue.2013.11.016 (2003).
54 Lisagor, W. B. (2005) Environmental cracking – stress corrosion, ASTM Corrosion Tests and Standards – Interpretation and Application (Manual 20).
55 Vasudevan, A. K. and Sadananda, K. (2009) Classification of environmentally assisted fatigue crack growth behavior. *Int. J. Fatig.*, **31**, 1696–1708.
56 Sadananda, K. and Vasudevan, A. K. (2011) Review of environmentally assisted cracking. *Metall. Mater. Trans. A*, **42**, 279–295.
57 Vasudevan, A. K. and Sadananda, K. (2011) Role of internal stresses on the incubation times during stress corrosion cracking. *Metall. Mater. Trans. A*, **42**, 396–404.
58 Vasudevan, A. K. and Sadananda, K. (2011) Role of slip mode on stress corrosion cracking behavior. *Metall. Mater. Trans. A*, **42**, 405–414.
59 Castro, J. T. P. and Meggiolaro, M. A. (2013) Is notch sensitivity a stress analysis problem? *Frattura ed Integrità Strutturale*, **25**, 79–86.
60 Sadananda, K. and Vasudevan, A. K. (2011) Failure diagram for chemically assisted crack. *Metall. Mater. Trans. A*, **42**, 296–303.
61 Sadananda, K. (2013) Failure diagram and chemical driving forces for subcritical crack growth. *Metall. Mater. Trans. A*, **44**, 1190–1199.